

Interferometric Observations of V838 Monocerotis

B. F. Lane¹, A. Retter², R. R. Thompson³, J. A. Eisner⁴

ABSTRACT

We have used long-baseline near-IR interferometry to resolve the peculiar eruptive variable V838 Mon and to provide the first direct measurement of its angular size. Assuming a uniform disk model for the emission we derive an apparent angular diameter of 1.83 ± 0.06 milli-arcseconds. For a nominal distance of 8 ± 2 kpc, this implies a linear radius of $1570 \pm 400 R_{\odot}$. However, the data are somewhat better fit by elliptical disk or binary component models, and we suggest that the emission may be strongly affected by ejecta from the outburst.

Subject headings: techniques:interferometric–star:V 838 Mon

1. Introduction

V838 Monocerotis is an eruptive variable star that underwent a nova-like event in early 2002 (Brown 2002; Munari et al. 2002), with a peak intensity of $m_V \sim 6.8$. However, the eruption was unlike classical novae in that the effective temperature of the object dropped and the spectral type evolved into a very late M–L type (Evans et al. 2003). Another unusual behavior was that the light-curve displayed multiple peaks in intensity, with the second peak being the brightest (Retter & Marom 2003). Spectroscopic studies indicated the presence of *s*-process elements, followed by the appearance of numerous oxygen-rich molecules (Lynch et al. 2004). The eruption mechanism of V838 Mon remains unclear, but appears to represent a new type of explosive variable. There have been two other variables that displayed similar

¹Center for Space Research, MIT Department of Physics, 70 Vassar Street, Cambridge, MA 02139; blane@mit.edu

²Astronomy & Astrophysics Dept., Penn State University, 525 Davey Lab, University Park, PA 16802-6305; retter@astro.psu.edu

³Michelson Science Center, 100-22 California Institute of Technology, Pasadena, CA 91125; thompson@ipac.caltech.edu

⁴Department of Astronomy, California Institute of Technology, MC 105-24, Pasadena, CA 91125; jae@astro.caltech.edu.

late, cool spectral properties: M31-RV (Rich et al. 1989; Mould et al. 1990; Bryan & Royer 1992) which achieved $M_V = -9.95$, and V4332 Sgr (Martini et al. (1999); $M_V \sim -4.5$ though the distance to V4332 Sgr is uncertain).

The discovery of a spectacular light-echo effect around V838 Mon (Henden et al. 2002) has allowed distance estimates to be made (Wisniewski, Bjorkman & Magalhaes 2003; Bond et al. 2003; Tylenda 2004; van Loon, Rushton & Smalley 2004); they indicate distances in the range 2.5 – 10 kpc, depending on the location of the reflecting material (circumstellar vs. interstellar.) It has been pointed out (Tylenda, Soker & Szczerba 2005) that the apparent center of the light echo appears to move on the sky; this is inconsistent with a circumstellar dust model and would appear to favor the interstellar interpretation. Assuming a distance of 8 ± 2 kpc (Tylenda 2004), the peak luminosity was $\sim 6.4 \times 10^5 L_\odot$ and the absolute visual magnitude was in the range $M_V \sim -7.7$ to -10 . As of late 2004 the source had dimmed considerably in the visible from peak intensity ($m_V = 14.82$; Kiss, personal communication to A.R.), but remained bright in the near-IR ($m_K = 5.52$; Ashok & Banerjee, 2004).

The progenitor of V838 Mon has been found (Munari, Desidera & Henden 2002; Wagner & Starrfield 2002; Kimeswenger et al. 2002; Goranskij et al. 2004) in a variety of surveys, including 2MASS (Beichman et al. 1998), and appears consistent with a somewhat reddened early main sequence star (B3V): $B = 15.8 \pm 0.06$, $K = 13.33 \pm 0.06$, $B - V \sim \pm 0.6$, $E_{B-V} \sim 0.77$. During the 66 years preceding the 2002 outburst the progenitor was not significantly variable (Goranskij et al. 2004). Kato et al. (2002) point out that the progenitor was detected by IRAS (IRAS 07015-0346). Post-outburst observations have found a faint, blue component in the spectrum (Desidera & Munari 2002; Wagner & Starrfield 2002) and Tylenda, Soker & Szczerba (2005) argued that the photometry is well-matched by a pair of early main sequence stars (B3V + B1.5V or B4V + A0.5V). Lynch et al. (2004) observed the IR behavior of V838 Mon and fit their data to a model consisting of a cool ($T_p = 2100$ K, $R_p = 8.8$ AU) stellar photosphere surrounded by a large, absorbing molecular cloud ($T = 850$ K, $R_c = 43$ AU), deriving a total mass of the ejecta of 0.03 – $0.13 M_\odot$.

Several models have been proposed to explain the outburst of V838 Mon. Initial models included thermonuclear runaway on an old, cool white dwarf (Iben & Tutukov 1992), though this may be hard to reconcile with the presence of a B3V companion. Another possibility is the merger of a pair of main-sequence binary stars (Soker & Tylenda 2003). It has also been suggested that V838 Mon is a post-AGB star and the event was due to He-flash (van Loon, Rushton & Smalley 2004). Finally, Retter & Marom (2003) have suggested that the eruption was due to the accretion of several close-in giant planets by an expanding giant or AGB star. This is consistent with the appearance of multiple peaks in the light curve, and with the spectroscopic detection of lithium (Munari et al. 2002).

We have used the Palomar Testbed Interferometer (PTI) to resolve the $2.2\mu\text{m}$ emission from V838 Mon and measure its apparent angular diameter. The Palomar Testbed Interferometer (PTI) was built by NASA/JPL as a testbed for developing ground-based interferometry and is located on Palomar Mountain near San Diego, CA (Colavita et al. 1999). It combines starlight from two 40-cm apertures and measures the resulting interference fringes. The high angular resolution provided by this long-baseline (85-110 m), near infrared ($2.2\mu\text{m}$) interferometer is sufficient to resolve emission on the milli-arcsecond scale. The measured apparent angular diameter can be combined with distance estimates from the light-echo to determine the size of the emitting region and thus help constrain explosion models.

2. Observations

We observed V838 Mon on 6 nights using PTI in the standard K-band mode, with the 85-meter North-West (4 nights) and South-West (2 nights) baselines. For detailed descriptions of the instrument we refer the reader to Colavita et al. (1999). Each nightly observation consisted of one or more 130-second integrations during which the normalized fringe visibility (or contrast) of the science target was measured. The measured fringe visibilities of the science target were calibrated by dividing them by the instrument point-source response of the instrument (typically ~ 0.75), determined by interleaving observations of calibration sources (Table 1); the calibration sources were chosen to be single stars with angular diameters smaller than 1 milli-arcsecond, determined by fitting a black-body to archival broadband photometry. While HD 49933 is listed as a double star in the SIMBAD database, the companion is faint ($m_V = 11.3$) and distant (~ 6 arcseconds) from HD 49933, giving it a negligible impact on the measured fringe visibilities. For further details of the data-reduction process, see Colavita (1999b) and Boden et al. (2000). Note that in addition to the uncertainties derived from the internal scatter in the data, we add a 5% minimum systematic uncertainty to the visibility measurements, consistent with worst-case estimates for PTI data based on comparisons with known sources.

PTI is equipped with a low-resolution spectrometer which provides fringe visibility measurements and photon count rates in five spectral channels across the K band. We compute a wide bandwidth average as the photon-weighted average of the five spectral channels. For the observations of V838 Mon, the photon rates in the two edge channels (2.0 and $2.4\mu\text{m}$) were too low to provide useful data, and thus the fringe visibilities are effectively measured from 2.1 to $2.3\mu\text{m}$. The faintness of the source in the edges of the K-band is consistent with the deep molecular absorption bands seen by Banerjee & Ashok (2002) using near-IR

spectroscopy. Using photon count rates from PTI, and K-band magnitudes for the calibrator sources provided by 2MASS (Beichman et al. 1998), we derive a K-band apparent magnitude of 5.45 ± 0.1 for V838 Mon, consistent with the measurement by Ashok & Banerjee (2004) of $m_K = 5.52 \pm 0.05$ made on 4 October 2004. We also note that within the limit of our statistical measurement noise (~ 0.06 mag) the apparent magnitude did not vary during the period of observations.

3. Results

The theoretical relation between source brightness distribution and fringe visibility is given by the van Cittert-Zernike theorem, with the two being a Fourier-transform pair. For a uniform intensity disk model the normalized fringe visibility can be related to the apparent angular diameter using

$$V^2 = \left(\frac{2 J_1(\pi B \theta_{UD} / \lambda)}{\pi B \theta_{UD} / \lambda} \right)^2 \quad (1)$$

where J_1 is the first-order Bessel function, B is the projected aperture separation, θ_{UD} is the apparent angular diameter of the star in the uniform-disk model, and λ is the wavelength of the observation. It is not necessarily true that the source is well-modeled by a uniform disk; it may be better modeled by a limb-darkened disk or even a Gaussian extended envelope (Perrin et al. 2004). However, there is insufficient data at this point to make meaningful comparisons between Gaussian and uniform disk models, and our uniform disk fits should be interpreted as measuring the angular extent of the source without providing detailed information on the radial intensity profile. On the other hand, the availability of data taken with two different baselines (and hence two different source position angles) provides information about the angular intensity profile, and in particular we are able to distinguish between a circularly symmetric source and elliptical models (see Eisner et al. (2003) for a discussion of simple emission models). As indicated in Figure 1 the NW and SW data sets give differing apparent diameters, indicating that the source is not circularly symmetric. We fit the combined (NW+SW) data set using an elliptical model and solve for major and minor-axis diameters and position angle. Another possible emission morphology is a pair of sources; we model such a binary source using standard expressions (Eisner et al. 2003) and fit for the binary separation, position angle and intensity ratio.

We performed least-squares fits of uniform disk, elliptical and binary models to the measured fringe visibilities. The results are given in Table 2 and Figure 1. We find that the circularly-symmetric uniform disk model does not match the data particularly well ($\chi^2_{d.o.f} = 1.7$, where $\chi^2_{d.o.f}$ is the sum of the squares of the residuals, divided by the number of degrees

of freedom). There is insufficient data to distinguish between an elliptical ($\chi^2_{d.o.f} \sim 1.2$) or a binary emission model ($\chi^2_{d.o.f} \sim 0.92$). It is likely that an even more complicated morphology will ultimately be required to fully match the data.

We examine the possibility of systematic errors mimicing the effect of non-symmetric emission using the following test: we use one of the calibrators (HD 49434) as a “check star”, calibrating it using our second calibrator (HD 49933), and fitting a circularly-symmetric uniform disk model (expected to be a good fit for a single main-sequence star) to this data set. The fit has $\chi^2_{d.o.f} = 1.4$ for 14 points (including points measured on both available baselines), and produces an apparent angular diameter of 0.39 ± 0.25 milli-arcseconds (data not shown), fully consistent with the expected diameter based on spectrophotometry. The large uncertainty in the final diameter is merely due to the fact that such a small source is very neary indistinguishable from a point source using the available baselines.

We would not expect to see the putative B3V binary companion to V838 Mon, as it would have a contrast ratio in the K band of ~ 10 magnitudes. Such a large magnitude difference would modulate the apparent fringe visibility by at most 10^{-8} , much smaller than our measurement precision.

4. Discussion

We have modeled the $2.2\mu\text{m}$ emission from V838 Mon using several simple emission morphologies, including uniform and elliptical disks and binary models. We find that the best fits to the data are provided by elliptical or binary models. However, the preference is not overwhelming. We also note that it is quite likely that the emission morphology is more complicated than these simple models indicate; further observations are certainly required. We caution the reader that the stated parameter uncertainties are merely indications of the statistical uncertainties. There is a larger, and less well-quantified, uncertainty associated with the choice of emission model.

If the emission is interpreted as coming from a circularly-symmetric uniform disk, the best-fit size is 1.83 ± 0.06 milli-arcseconds. For a distance of 8 ± 2 kpc, derived from the light-echo, the implied linear radius is 7.3 ± 1.8 AU ($1570 \pm 400R_\odot$) Such a large stellar radius is consistent with previous estimates made during the outburst based on fitting an emission model to spectro-photometry: Lynch et al. (2004) derive a stellar photosphere radius of 5.6 AU, assuming a distance of 6 kpc. Scaling that result to a distance of 8 kpc would imply an apparent radius of 7.5 AU. Such a large radius cannot be the radius of the white dwarf. In a nova outburst the system returns to its normal dimension in a few weeks or months -

much less than the 3 years elapsed before our observations (Hauschildt et al. 1997; Retter, Leibowitz & Ofek 1997; Retter 1999).

It is interesting to compare the measured apparent radius with what might be expected based on simple photometric models: if we fit a black-body model to the observed near-contemporaneous JHK magnitudes (October 2004; Ashok & Banerjee 2004) we derive a temperature of $T = 1950 \pm 100$ K, a bolometric luminosity of $\sim 30000L_\odot$ and an apparent angular diameter of $\theta = 1.3 \pm 0.6$ milli-arcseconds, marginally consistent with our measured value. However, a black-body is not a particularly suitable model for a 2000K stellar atmosphere. A better approximation can be provided by empirical surface-brightness relations. Using the same photometry, and assuming a reddening correction $A_V = 2.3$ together with V- and K-band surface-brightness relations from Groenewegen (2004) the available photometry predicts apparent angular diameters in the range $\sim 0.6 - 0.7$ milli-arcseconds. However, it should be noted that the $J - K$ color (~ 1.5) is somewhat out of the range of colors used to derive the relation (-0.2–1.3).

The best formal fit to the data is given by a binary source model. However, this result must be interpreted with caution. The intensity ratio between the components, though uncertain, is nearly equal ($R = 0.43^{+0.57}_{-0.34}$) in the K-band. Given that the K-band emission is dominated by a single cool blackbody that appeared after the outburst, it is hard to imagine a scenario where the two sources are not ultimately the result of a single outburst mechanism. The best-fit separation of the binary components is $5.51^{+5.5}_{-0.13}$ milli-arcseconds (44.1^{+42}_{-1} AU). Another possibility indicated by the data is that the observed K-band emission is produced by a very elongated, elliptical structure. The projected linear dimensions of such a source are approximately $3.5^{+0.2}_{-1.5} \times 0.07^{+3.0}_{-0.07}$ milli-arcseconds ($28^{+2}_{-13} \times 0.5^{+24}_{-0.6}$ AU).

We suggest that the observed K-band emission may be in part due to ejecta produced during the eruption. Soon after the peak of the outburst, the expansion velocity of the ejecta was estimated as 50–350 km/s (Munari et al. 2002; Crause et al. 2003; Kipper et al. 2004). For the time elapsed since outburst of $\sim 10^8$ s, the distance between the ejecta and the star should be in the range 30–220 AU. This range is consistent with the projected separations we measure. It is also likely that the ejecta are not uniformly distributed, and hence the binary morphology preferred by the data may be “clumpiness” in the ejecta. In this context we note that polarimetric observations during the outburst (Desidera et al. 2004) indicate that the source became significantly polarized (0.7% at 5000Å). This has been interpreted as being due to departures from spherical symmetry during the outburst.

5. Conclusion

We have used the Palomar Testbed Interferometer to observe the peculiar outbursting variable V838 Mon. This is only the second published observation of a nova-like outburst using an optical/near-IR interferometer - the only previous result being the observations of Nova Cyg 1992 done using the Mk III interferometer (Quirrenbach et al. 1993). The high angular resolution provided by PTI allows us to draw two preliminary conclusions. First, the source is resolved by our instrument and has a characteristic angular size of a few milli-arcseconds. Second, the difference in measured fringe visibility between the two baselines is inconsistent with the source being a simple uniform disk. We have explored other possible source morphologies, including inclined disks and binary models and find that the data can be reasonably matched by such models, but clearly further data are needed to constrain them. We point out that any of the models proposed to explain the outburst of V838 Mon need to account for the presence of very extended, cool, non-symmetric emission.

We wish to acknowledge the extraordinary efforts of K. Rykoski, and to thank an anonymous referee for helpful comments. Observations with PTI are made possible through the efforts of the PTI Collaboration, which we acknowledge. This research has made use of the Michelson Science Center at Caltech (<http://msc.caltech.edu>), JPL/NASA, the Simbad database CDS (Strasbourg, France), and of data products from the Two Micron All Sky Survey, which is a joint project of the University of Massachusetts and the IPAC/Caltech, funded by NASA and NSF. BFL acknowledges support from a Pappalardo Fellowship in Physics and JAE is grateful for a Michelson Graduate Fellowship.

REFERENCES

Ashok, N. M. & Banerjee, D. P. K. 2004, IAU Circ., 8423, 2

Banerjee, D. P. K. & Ashok, N. M. 2002, A&A, 395, 161

Beichman, C. A., Chester, T. J., Skrutskie, M., Low, F. J., & Gillett, F. 1998, PASP, 110, 480

Boden, A., Creech-Eakman, M., Queloz, D., 2000, ApJ, 536, 880-890.

Bond, H. E., et al. 2003, Nature, 422, 405

Boschi, F., Munari, U. 2004, A&A, 418, 869

Brown, N. J., 2002, IAUC 7785.

Bryan, J., Royer, R. E. 1992, PASP, 104, 179

Colavita, M. M., et al. 1999, ApJ, 510, 505.

Colavita, M. M., 1999, PASP, 111, 111.

Crause, L. A., Lawson, W. A., Kilkenny, D., van Wyk, F., Marang, F., & Jones, A. F. 2003, MNRAS, 341, 785

Desidera, S., & Munari, U. 2002, IAU Circ., 7982, 1

Desidera, S., et al. 2004, A&A, 414, 591

Eisner, J. A., Lane, B. F., Akeson, R. L., Hillenbrand, L. A., & Sargent, A. I. 2003, ApJ, 588, 360

Evans, A. et al. 2003, MNRAS, 343, 1054

Goranskij, V. P., Shugarov, S. Y., Barsukova, E. A., & Kroll, P. 2004, IBVS, 5511, 1.

Groenewegen, M. A. T. 2004, MNRAS, 353, 903

Hauschildt, P. H., Shore, S.N., Schwarz, G.J., Baron, E., Starrfield, S. & Allard, F., 1997, ApJ, 490, 803

Henden, A., Munari, U., & Schwartz, M.B., 2002, IAUC, 7859.

Iben, I. J., & Tutukov, A. V. 1992, ApJ, 389, 369

Kato, T., Yamaoka, H., & Kiyota, S. 2002, IAU Circ., 7786, 3

Kimeswenger, S., Lederle, C., Schmeja, S., & Armsdorfer, B. 2002, MNRAS, 336, L43

Kipper, T., et al. 2004, A&A, 416, 1107

Lynch, D. K. et al. 2004, ApJ, 607, 460

Martini, P., Wagner, R. M., Tomaney, A., Rich, R. M., della Valle, M., & Hauschildt, P. H. 1999, AJ, 118, 1034

Mould, J. et al. 1990, ApJ, 353, L35

Munari, U., Desidera, S., & Henden, A., 2002, IAUC, 8005

Munari, U. et al. 2002, A&A, 389, L51

Perrin, G., et al. 2004, A&A, 426, 279

Quirrenbach, A., Elias, N. M., Mozurkewich, D., Armstrong, J. T., Buscher, D. F., & Hummel, C. A. 1993, AJ, 106, 1118

Retter, A., Leibowitz, E. M., & Ofek, E. O. 1997, MNRAS, 286, 745

Retter, A. 1999, PASP, 111, 774

Retter, A., & Marom, A. 2003, MNRAS, 345, L25

Retter, A., Zhang, B., Siess, L., & Levinson, A. 2004, ApJ, submitted

Rich, R. M., Mould, J., Picard, A., Frogel, J. A., & Davies, R. 1989, ApJ, 341, L51

Soker, N., & Tylenda, R. 2003, ApJ, 582, L105

Tylenda, R. 2004, A&A, 414, 223

Tylenda, R., Soker, N. & Szczerba, 2005, astro-ph/0412183.

Van Loon, J. Th., Evans, A., Rushton, M. T., & Smalley, B. 2004, A&A, 427, 193

Wagner, R. M., & Starrfield, S. 2002, IAUC, 7992

Wisniewski, J.P., Bjorkman, K. S., Magalhaes, A. M., 2003, ApJ, 598, L43-46.

Calibrator	V	K	Spectral Type	Ang. Diameter θ_{UD} (mas)	Separation (deg)
HD 49434	5.75	5.01	F1V	0.36 ± 0.1	4.7
HD 49933	5.78	4.72	F2V	0.42 ± 0.1	4.7

Table 1: Relevant parameters of the calibrators. The separation listed is the angular distance from the calibrator to V838 Mon.

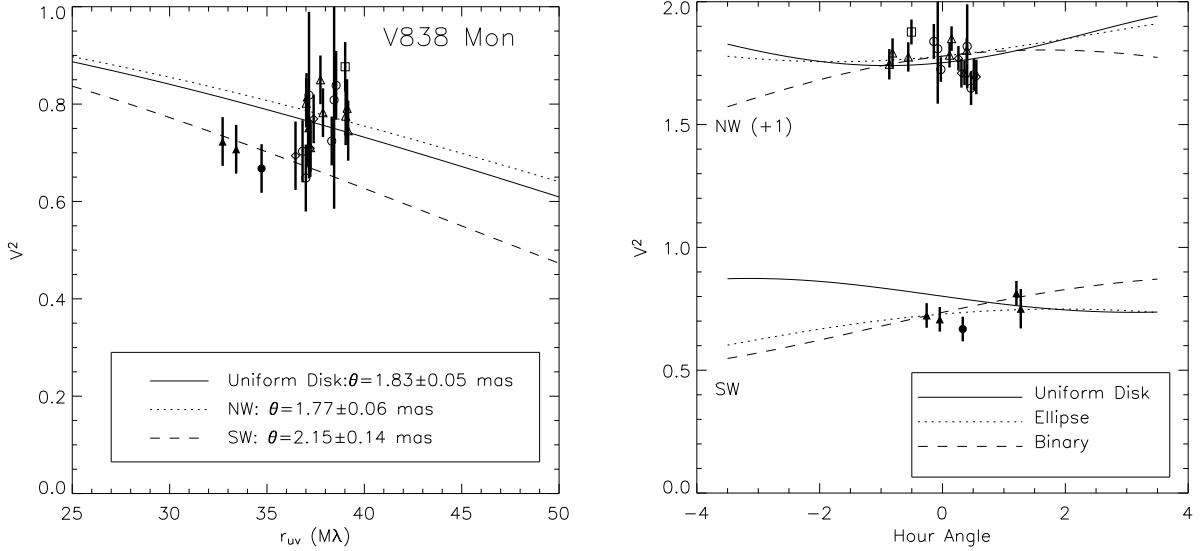


Fig. 1.— Left: The measured fringe visibility (V^2) of V838 Mon as a function of projected baseline length measured in units of the observing wavelength ($2.2\mu\text{m}$). Different symbols are used for different nights. Filled symbols are used for data taken with the South-West baseline, open symbols indicate North-West baseline data. Best-fit uniform-disk models are shown for combined and single-baseline data sets. The data show that the emission is resolved and is inconsistent with an circularly symmetric emission source. Right: The measured fringe contrast as a function of source hour angle, together with the best-fit models. A binary or inclined disk model is required to account for the data from both baselines. Note that the NW-baseline data have been moved up by 1.0 for clarity.

Model	χ^2_r	Size (mas)	Pos. Angle (deg)	Minor axis or intensity ratio.
Uniform Disk	1.7	$1.83^{+0.06}_{-0.06}$	—	—
Elliptical	1.3	$3.57^{+0.22}_{-1.56}$	15^{+3}_{-27}	$0.07^{+3.03}_{-0.07}$
Binary Model	0.9	$5.51^{+5.2}_{-0.13}$	36^{+3}_{-27}	$0.43^{+0.57}_{-0.34}$

Table 2: Fits of various emission models for V838 Mon. Size refers to the characteristic angular variable: angular diameter for a uniform disk, major-axis diameter for the elliptical model, and separation angle for the binary model. For the case of a binary model, the last column lists the component intensity ratio, R , while for the elliptical model the minor-axis diameter is given. The errors have been scaled by $\sqrt{\chi^2_{d.o.f.}}$. Note that the position angle has a 180-degree ambiguity.